INVESTIGATION OF THE COAGULATION AND ADHESION PHENOMENA IN COLLOIDS BY FIELD-FLOW FRACTIONATION

A. Koliadima[a]; D. Gavril[a]; G. Karaiskakis[a]

[a] Department of Chemistry, University of Patras, Patras, Greece

PLEASE SCROLL DOWN FOR ARTICLE

INVESTIGATION OF THE COAGULATION AND ADHESION PHENOMENA IN COLLOIDS BY FIELD-FLOW FRACTIONATION

A. Koliadima,* D. Gavril, G. Karaiskakis

Department of Chemistry
University of Patras
GR-26500, Patras, Greece

ABSTRACT

Conventional and potential barrier methodologies of Field-Flow Fractionation are used to separate and characterize colloidal particles of haematite and titanium dioxide.

The colloidal particles are reversibly adsorbed at the beginning of the Sedimentation Field-Flow Fractionation channel wall. The reversibility of the adsorption of these particles can be achieved by the appropriate adjustment of various parameters among which the must suitable is the ionic strength of the carrier solution.

In the present work by using both Field-Flow Fractionation (FFF) and Transmission Electron Microscopy (TEM) techniques we investigate whether the reversible adsorption of the haematite and titanium dioxide particles on the stainless-steel channel wall is due to their reversible coagulation or to the variation of the interaction forces between the colloidal particles and the solid surface.

INTRODUCTION

In Field-Flow Fractionation (FFF) components are separated due to their differential interaction with an applied field.[1-4] Sedimentation Field-Flow Fractionation (SdFFF) is capable of separating and characterizing colloidal and particulate materials.[5, 6] It is a relatively new technique for the high resolution separation and analysis of a wide variety of colloids and macromolecules.[3-6]

Samples are separated in a thin channel on the basis of their effective masses. The flow through the channel has a parabolic profile whose flow velocity approaches zero at both walls and reaches a maximum at the midpoint between the walls. When a centrifugal force is applied across the channel, particles are driven toward the bottom wall, and an equilibrium distribution is established between the external force and diffusion of the particles.[5] Since the equilibrium distribution will determine the average velocity for a sample zone eluted through the channel, the sample particles elute in order of decreasing diffusion coefficient, i.e. the smaller particles elute first. When the average distance from the accumulation wall is exceeded by the particle radius, the steric-hyperlayer effect has to be considered and the particle velocity will increase with increasing diameter. As a consequence, the onset of the steric mechanism causes a shift in the elution order, so that the larger particles elute first.[7-9]

Potential-barrier Field-Flow Fractionation (PBFFF) is a new method,[10,11] which is based either on particle size differences or on Hamaker constant, surface potential[12,14] and Debye-Huckel reciprocal distance differences. Experimentally, this should be done by changing the ionic strength of the carrier solution[10,11] from a high value, in which the colloidal particles are adsorbed at the beginning of the SdFFF channel wall, to a lower value, where the total number of adhered particles is released.[10, 11, 15, 16]

The PBFFF technique can be used successfully to separate and characterize dilute and concentrated colloidal samples even with the same size but with different limiting electrolyte concentrations for their adsorption on solid surfaces.

In the present work we investigated whether the reversible adsorption of the colloidal particles on the stainless-steel channel wall is due to their reversible coagulation or to the interaction forces between the colloids and the solid surface.

EXPERIMENTAL

The basic sedimentation FFF system used for these studies has been described in detail previously.[13, 17, 18] Three channels having different dimensions

were used in the present work. The first (channel-1) had a length of 38.4 cm, breadth of 2.05 cm, and thickness of 0.0262 cm. The void volume of the channel-1 measured by the elution of non-retained peak of sodium benzoate was found to be 2.06 cm^3. The second channel (channel-2) had the following dimensions: $38.5 \times 2.3 \times 0.0181$ cm^3 with a channel void volume of 1.60 cm^3. The third channel (channel-3) had breadth of 2.35 cm, thickness of 0.0193 cm and the same length as the channel-1. The void volume, measured by the same method, was 1.74 cm^3.

In all systems the column was 6.85 cm from the centre of rotation. A Gilson Holochrome UV detector was used for detection at 254 nm and a Gilson Minipuls 2 peristaltic pump was used to pump the carrier solution and the sample to the channels.

Titanium dioxide monodisperse colloidal particles from PolySciences with an average diameter of d = 0.310 μm (obtained by TEM), which were studied in channel-1, and haematite nearly monodisperse colloidal particles of two sizes provided by Prof. J. Lyklema (Agricultural University, Wageningen, The Netherlands) with an average diameter (obtained by TEM) of d = 0.146 μm [a-Fe$_2$O$_3$(I)] and d = 0.258 μm [a-Fe$_2$O$_3$(II)], which were studied in channels 2 and 3, respectively, were used as samples. The morphology of the sample particles were investigated by Phillips CM-20 transmission electron microscopy (TEM) at 200 kV.

The carrier solution was triply distilled water containing 0.5% (v/v) of detergent FL-70 (Fisher Scientific Co.) and 0.02% (w/w) sodium azide as bacteriocide. Potassium nitrate from Riedel-De Haen A.G., was added to the carrier solution for the adjustment of the ionic strength.

The experimental procedure was described in detail elsewhere.[11]   The critical electrolyte (KNO$_3$) concentration of the carrier solution for the total adsorption of TiO$_2$ and a-Fe$_2$O$_3$ (II) on the stainless-steel channel was found to be 3×10^{-2} M, while that for the adsorption of a-Fe$_2$O$_3$(I) particles was found to be 8×10^{-2}M.

RESULTS AND DISCUSSION

The basic retention relationship in FFF shows that the retention ratio R is a function only of the dimensionless retention parameter λ[3, 19, 20]:

$$R = 6\lambda\left[\coth\left(1/2\lambda\right) - 2\lambda\right] = \frac{V_o}{V_r} \tag{1}$$
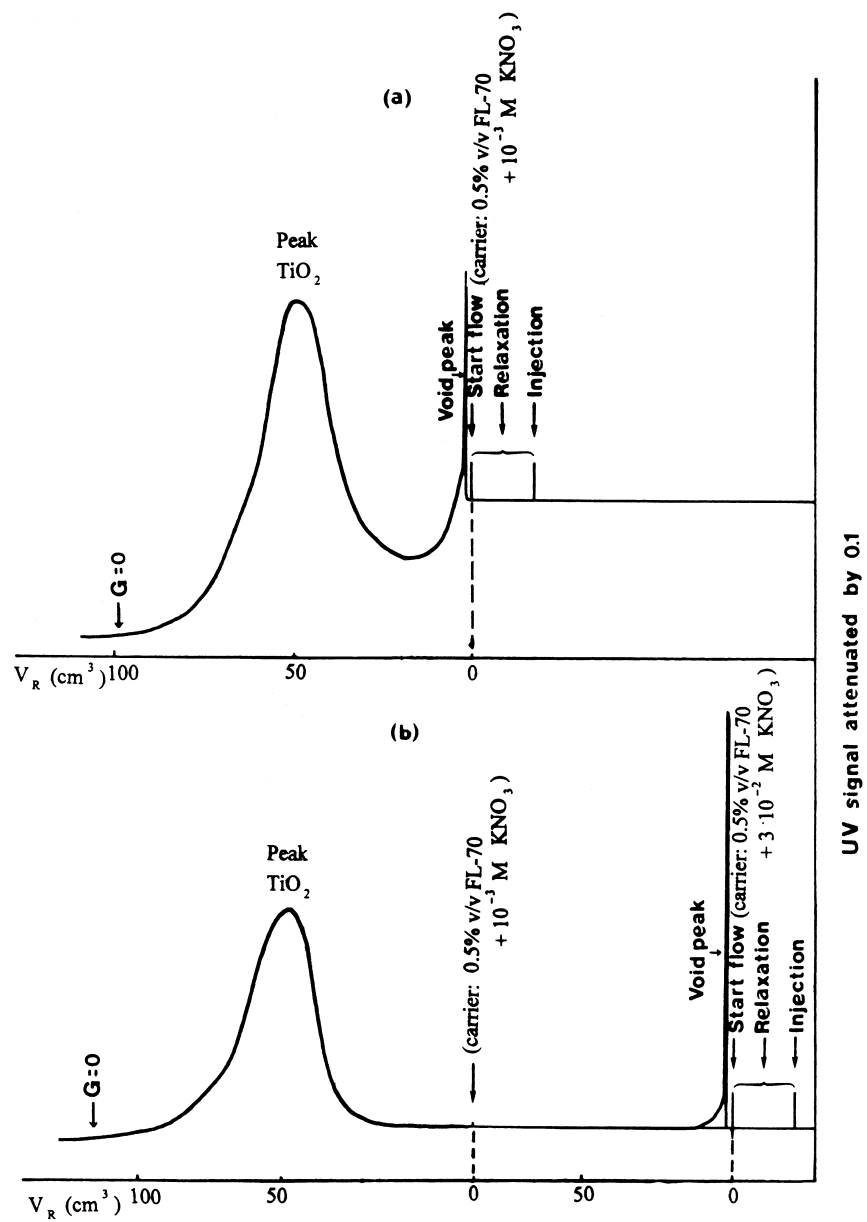
Figure 1. Fractograms of monodisperse TiO_2 spherical particles obtained (a) by conventional sedimentation FFF and (b) by potential barrier sedimentation FFF.
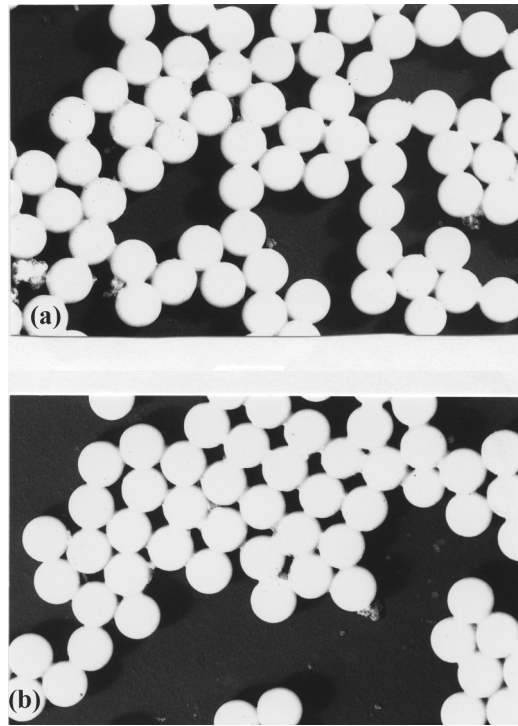
Figure 2. Transmission electron micrographs (TEMs) of TiO$_2$ particles (20000x) dispersed (a) in 0.5% v/v FL-70 + 1 × 10^{-3} M KNO$_3$ and (b) in 0.5% v/v FL-70 + 3 × 10^{-2} M KNO$_3$.

where V_o is the channel void volume and V_r is the retention volume of retained particles.

When $\lambda << 1$, Equation (1) reduces to the simple limiting form:

$$\lim_{\lambda \to 0} R \approx 6\lambda \tag{2}$$

In conventional Sedimentation FFF (SdFFF), where the interactions between the colloidal particles and the channel wall are absent, any observed

value of V_r or R can be converted into the diameter d of a spherical particle via the equation:

$$d = \left(\frac{36kTV_r}{\pi Gw\Delta\rho V_o} \right)^{1/3} \tag{3}$$

where k is Boltzmann's constant, T is absolute temperature, G is the field strength expressed as acceleration, w is the channel thickness and $\Delta\rho$ is the density difference between the particles and the carrier solution.

In Potential Barrier FFF (PBFFF) by changing the total potential energy of interaction between the colloidal particles and the channel wall one can succeed the adhesion of the whole number of colloidal particles on the solid surface, which can be followed by the release of the adhered particles. Experimentally, this can be done by changing the surface potential of the particles, ψ_1, or the Hamaker constant, A, and the Debye-Huckel reciprocal distance, $\kappa^{-1} = BI^{1/2}$, as the total potential energy, U, of a spherical particle is given by the expression:[11]

$$\begin{aligned} U = {} & \frac{4}{3}\pi r^3 \Delta\, Gx + \frac{A}{6}\left[\ln\left(\frac{H+2r}{H} \right) - \frac{2r(H+r)}{H(H+2r)} \right] \\ & + 16\varepsilon\, r\left(\frac{kT}{e} \right)^2 \tan h\left(\frac{e_1\psi_1}{4kT} \right) \tan h\left(\frac{e\psi_2}{4kT} \right) e^{\frac{H}{BI^{1/2}}} \end{aligned} \tag{4}$$

where r is the particle radius, x is the coordinate position of the centre of particle mass, H is the separation distance between the sphere and the channel wall, M is the dielectric constant of the liquid phase, e is the electronic charge, ψ_2 is the surface potential of the solid surface, B is a constant and I is the ionic strength of the carrier solution. In its simplest form the PBFFF technique consists in changing the ionic strength of the carrier solution from a high value, where the attraction between the colloidal particles and the channel leads to the total adsorption of the particles at the beginning of the SdFFF channel wall, to a lower value, where the total number of adhered particles is released.

In the present work the PBFFF technique was applied to the monodisperse spherical particles of titanium dioxide, as well as to the nearly monodisperse spherical particles of haematite. Figure 1a shows a fractogram obtained by the conventional SdFFF technique for the TiO_2 sample suspended in a carrier solution containing a low concentration of potassium nitrate (ca. 1×10^{-3} M). The retention volume was found to be 49.1 cm^3 and calculated with the aid of
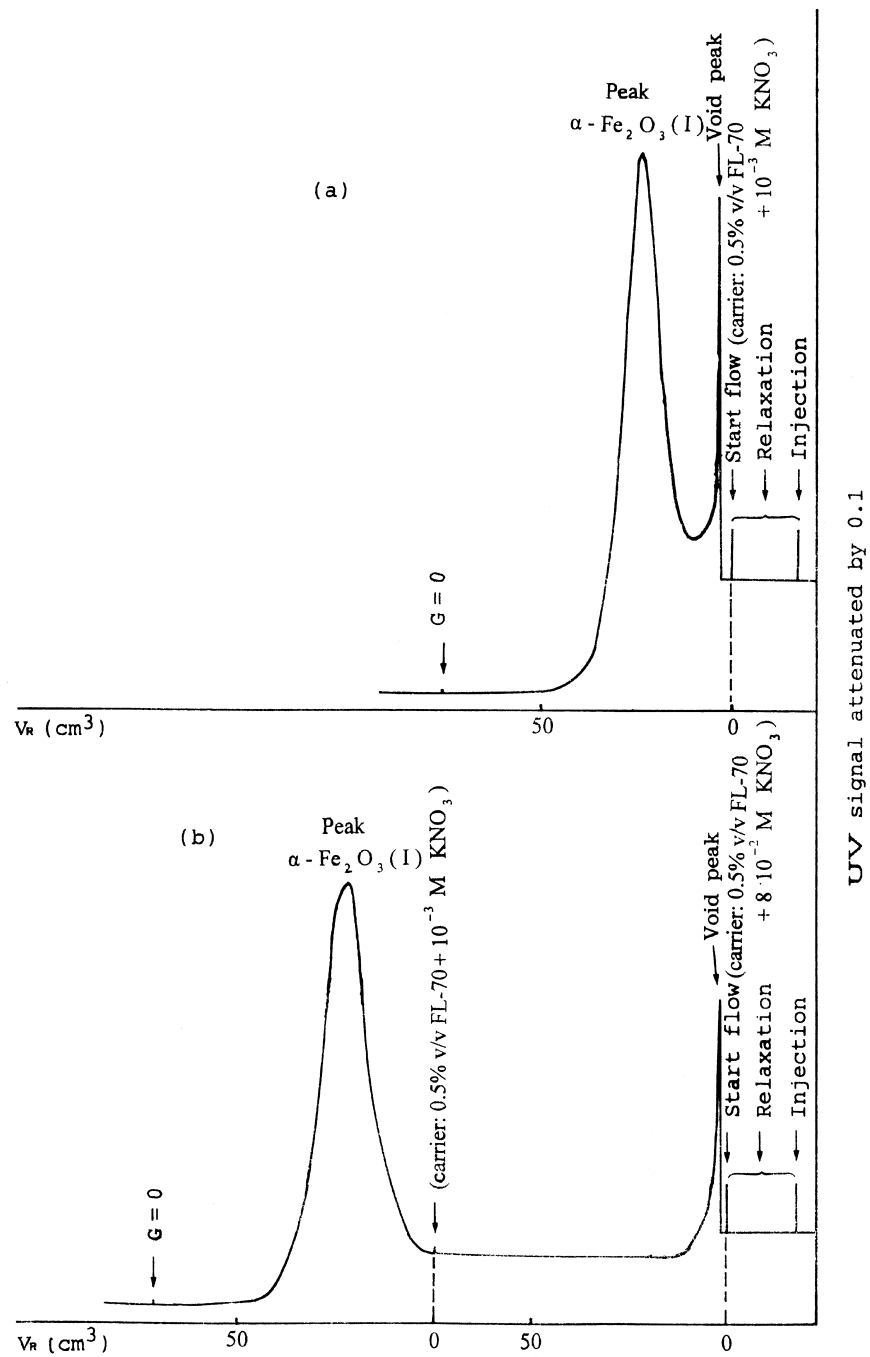
Table 1

**Particle Diameters for the Sample of TiO_2, a-Fe_2O_3(I) and a-Fe_2O_3(II)
Obtained by Transmission Electron Microscope at Various Dispersing
Solutions**

Dispersing Solution	Particle Diameter (μm)		
	TiO_2	a-Fe_2O_3(I)	a-Fe_2O_3(II)
0.5% v/v FL-70	----	0.145	0.258
0.5% v/v FL-70 + 1×10^{-3} M KNO_3	0.310	0.146	0.258
0.5% v/v FL-70 + 3×10^{-2} M KNO_3	0.309	----	0.248
0.5% v/v FL-70 + 8×10^{-2} M KNO_3	----	0.142	----

Equation (3) diameter was 0.310 μm. Changing the carrier solution to the one containing higher concentration of KNO_3 (ca. 3×10^{-2} M) led to the adsorption of the whole particle of TiO_2 on the channel wall. Finally, changing again the concentration of the carrier solution to the original one (ca. 1×10^{-3} M) led to the appearance of a sample peak, due to the desorption of the adhered particles (cf. Figure 1b).

The retention volume of this sample peak was 48.4 cm^3 and the calculated particle diameter was found to be 0.309 μm, very close to that found (0.310 μm) from the direct injection of TiO_2 particles into the channel by the conventional SdFFF technique.   The release of all the adhered TiO_2 particles during the PBFFF procedure was verified by the fact that no elution peak was obtained when the field strength was reduced to zero.

In order to show whether the adhesion of the TiO_2 particles on the channel wall is due to the their reversible coagulation, during the variation of the carrier solution ionic strength, TEM pictures for the TiO_2 sample dispersed in two different solutions were received (cf. Figure 2). The first solution contained detergent FL-70 (0.5% v/v) with 1×10^{-3} M KNO_3, in which no adsorption of the particles was observed, while the second detergent FL-70 (0.5% v/v) with 3×10^{-2} M KNO_3, in which the total number of TiO_2 particles is adhered at the beginning of the channel wall. The TEM pictures show that the TiO_2 particles have the same shape and size in both solutions (0.310 μm in the carrier solution with 1×10^{-3} M KNO_3 and 0.309 μm in the carrier solution with 3×10^{-2} M KNO_3, cf. Table 1).

(a)

Peak
α - Fe$_2$O$_3$ (I)

Void peak

Start flow (carrier: 0.5% v/v FL-70 + 10^{-3} M KNO$_3$)

Relaxation

Injection

G = 0

V$_R$ (cm^3)

50   0

(b)

Peak
α - Fe$_2$O$_3$ (I)

(carrier: 0.5% v/v FL-70 + 10^{-3} M KNO$_3$)

Void peak

Start flow (carrier: 0.5% v/v FL-70 + 8·10^{-2} M KNO$_3$)

Relaxation

Injection

G = 0

V$_R$ (cm^3)

50   0   50   0

UV signal attenuated by 0.1

These values, which were measured from about 20 spheres in the TEM pictures, are exactly the same with those found by the PBFFF technique (0.309 µm) or the conventional SdFFF technique (0.310 µm) by the direct injection of TiO$_2$ particles into the channel, indicating that no reversible aggregation takes place during the variation of the ionic strength of the suspending medium. Thus, the total adhesion of the TiO$_2$ particles on the channel wall at concentrations of KNO$_3$ higher than 3×10^{-2} M can be attributed to the strong energy of attraction between the colloidal particles and the solid surface, which increases with the electrolyte concentration [cf. Equation (4)], and not to the coagulation of particles. It is obvious from Equation (3) that the increase of particle diameter due to the aggregation process leads to a higher increase in the retention volume. Thus the particles are moved along the column with a such low velocity, so that one could approximately consider that the particles are adhered at the beginning of the SdFFF channel wall.

The same phenomenon was investigated by using two samples of haematite [a-Fe$_2$O$_3$(I) with d = 0.146 µm and a-Fe$_2$O$_3$(II) with d = 0.258 µm] with nearly monodisperse spherical particles. Figure 3a shows a fractogram for the a-Fe$_2$O$_3$(I) sample obtained by the conventional SdFFF technique at a low electrolyte concentration (ca. 1×10^{-3} M KNO$_3$), in which no adsorption of the colloidal particles takes place at the beginning of the channel wall. The retention volume was found to be 24.8 cm^3, which corresponds to a particle diameter of 0.146 µm.

Changing the carrier solution to one containing a higher concentration of KNO$_3$ (ca. 8×10^{-2} M) led to the adsorption of all the a-Fe$_2$O$_3$(I) particles on the stainless-steel channel wall, as no elution curve was observed. When the carrier solution was changed to one containing a lower ionic strength (ca. 1×10^{-3} M KNO$_3$), a sample peak appeared as a consequence of the desorption of the a-Fe$_2$O$_3$(I) particles (cf. Figure 3b). The mean diameter of the a-Fe$_2$O$_3$(I) particles (0.148 µm) is very close to that obtained by the conventional SdFFF (0.146 µm), in which no adsorption of the colloidal particles takes place at the beginning of the channel wall.

The investigation of the adhesion process of the a-Fe$_2$O$_3$(I) particles on the SdFFF channel wall was done again by using the TEM technique. TEM pictures of the a-Fe$_2$O$_3$(I) particles dispersed in three different solutions (ca. 0.5% v/v FL-70, 0.5% v/v FL-70 + 1×10^{-3} M KNO$_3$ and 0.5% v/v FL-70 + 8×10^{-2} M KNO$_3$) were received (cf. Figure 4).

Figure 3 (left). Fractograms of a-Fe$_2$O$_3$(I) colloidal particles obtained (a) by conventional sedimentation FFF and (b) by potential barrier sedimentation FFF.
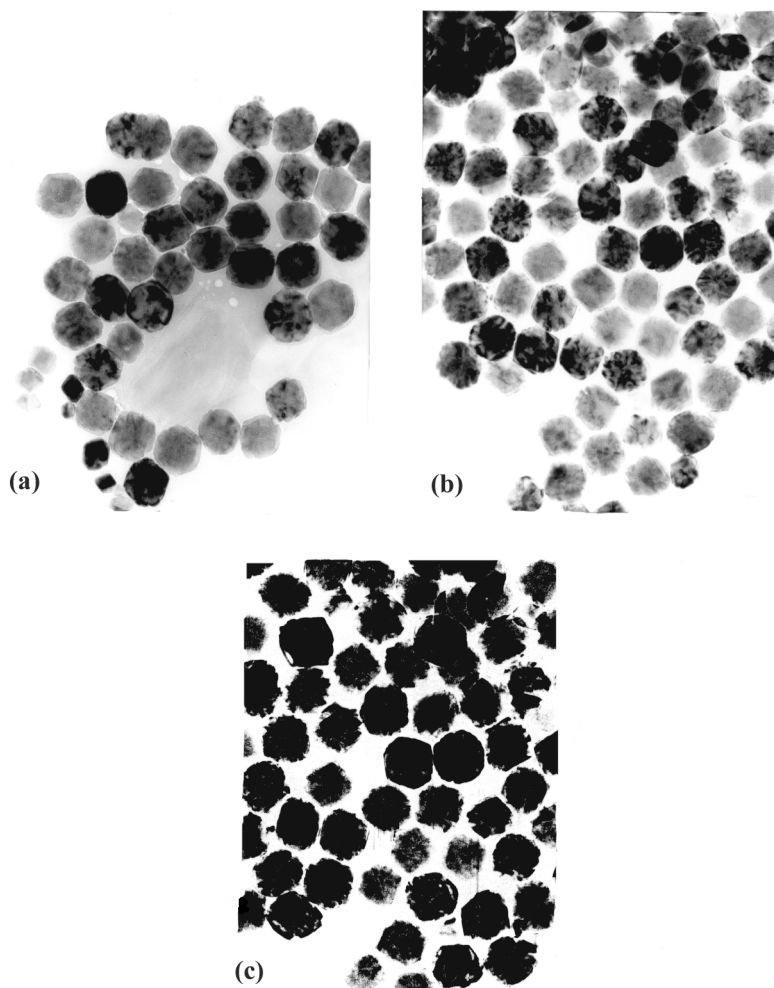
Figure 4. Transmission electron micrographs (TEMs) of a-Fe$_2$O$_3$(I) particles (50000 x) dispersed (a) in 0.5% v/v FL-70 (b) in 0.5% v/v FL-70 + 10^{-3} M KNO$_3$ and (c) in 0.5% v/v FL-70 + 8 × 10^{-2} M KNO$_3$.

The resulting mean diameters by measuring the size of about twenty (20) spheres in the TEM pictures, which are given in Table 1, are very close to each other, as well as to those determined by the conventional SdFFF (0.146 μm) and the PBFFF (0.148 μm) technique. The latter indicates that no aggregation of the
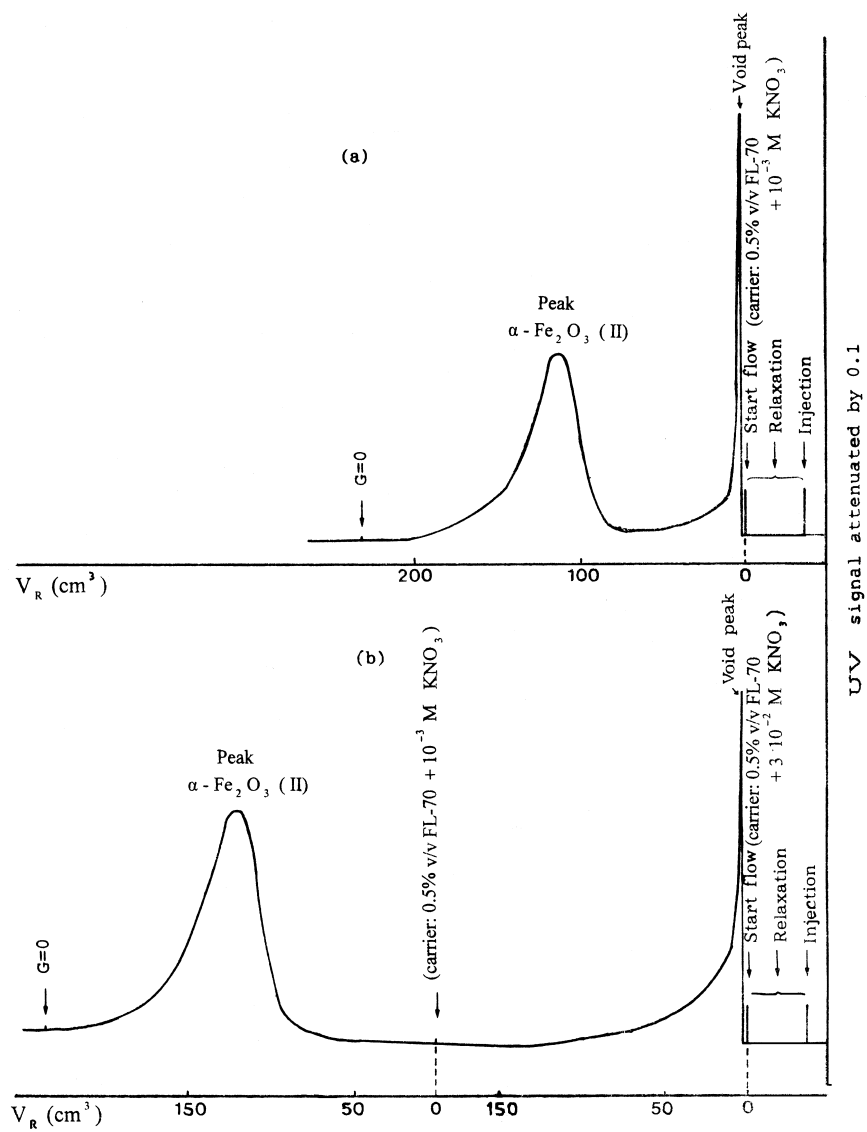
Figure 5. Fractograms of a-Fe$_2$O$_3$(II) colloidal particles obtained (a) by conventional sedimentation FFF and (b) by potential barrier sedimentation FFF.

(a)

(b)

(c)

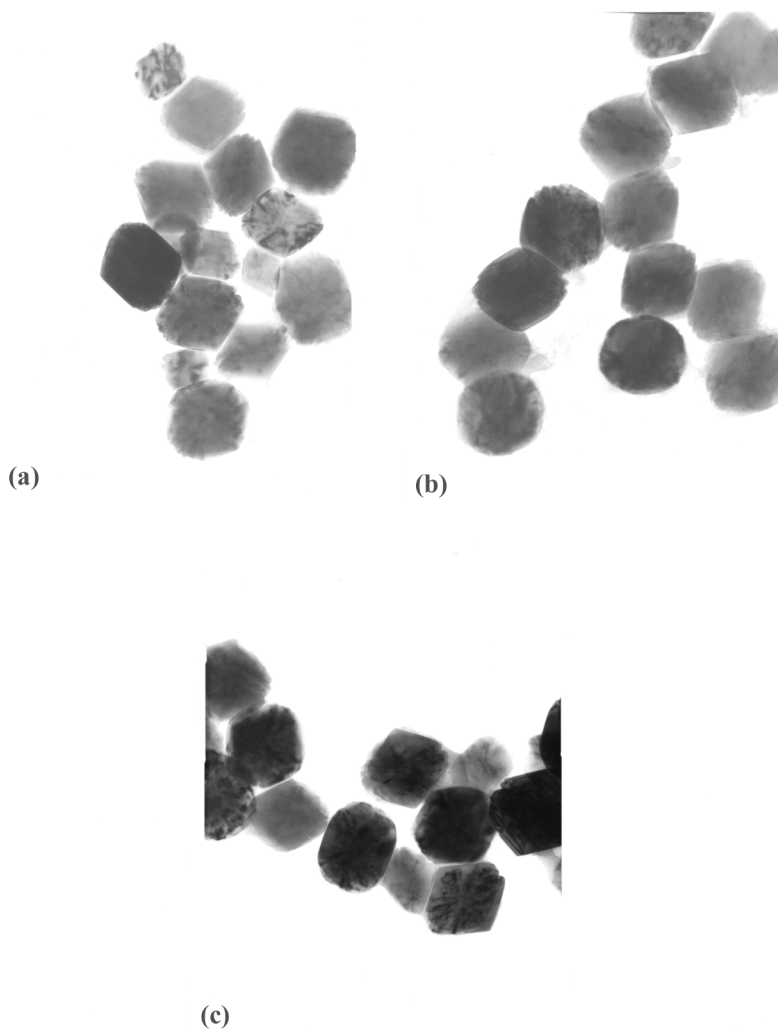**Figure 6**. Transmission electron micrographs (TEMs) of a-Fe$_2$O$_3$(II) particles (50000 x) dispersed (a) in 0.5% v/v FL-70 (b) in 0.5% v/v FL-70 + 10^{-3} M KNO$_3$ and (c) in 0.5% v/v FL-70 + 3 × 10^{-2} M KNO$_3$.

a-Fe$_2$O$_3$(I) particles occurs at the dispersing medium with the higher electrolyte concentration (8 × 10^{-2} M KNO$_3$) in which adsorption of the whole number of haematite particles takes place at the beginning of the SdFFF channel wall. Thus, the adhesion of a-Fe$_2$O$_3$(I) particles on the solid surface is due, as it was

also explained for the TiO_2 particles, to the increase of the van der Waals attraction potential, because of the increase of the ionic strength of the dispersing medium [cf. Equation (4)].

Finally, in order to show whether the particle size influences the total interaction potential between a spherical particle and a solid surface, as Equation (4) shows, we used a second sample of the same haematite material, a-Fe_2O_3(II), but with different particle diameter d = 0.258 μm. Following the procedure described in the analysis of the previous two samples [TiO_2 and a-Fe_2O_3(I)], we found for the a-Fe_2O_3(II) sample a particle diameter of 0.245 μm by the conventional SdFFF technique, exactly the same as that determined by the PBFFF technique (cf. Figure 5). The critical electrolyte concentration at which adsorption of all of the a-Fe_2O_3(II) colloidal particles occurs, at the beginning of the column was found to be 3×10^{-2} M KNO_3, [significantly lower from the value 8×10^{-2} M KNO_3 found for the adhesion of a-Fe_2O_3(I) particles], while that at which the total number of adherent a-Fe_2O_3(II) particles is released was 1×10^{-3} M KNO_3.

The measured mean particle diameters of the a-Fe_2O_3(II) sample at three different carrier solutions, (from the TEM pictures, cf. Figure 6) which are given in Table 1, are very close to each other (0.258 μm for the carrier solution (c.s.) with only 0.5% v/v FL-70, 0.258 μm for the c.s. with 0.5% v/v FL-70 + 1 $\times$ 10^{-3} M KNO_3 and 0.248 μm for the c.s. with 0.5% v/v FL-70 + 3×10^{-2} M KNO_3), as well as to those determined by the conventional SdFFF (0.245 μm) and PBFFF (0.245 μm) techniques. The latter indicates that during adhesion no aggregation phenomena of a-Fe_2O_3(II) particles take place and their total adsorption on the solid surface at high electrolyte concentrations can be attributed to the increase of the van der Waals attraction potential between the a-Fe_2O_3(II) particles and the sedimentation FFF channel wall.

In conclusion, although the TEM process suffers from the disadvantage of destroying the particle environment, the combination of the Field-Flow Fractionation technique with the Transmission Electron Microscopy method gives invaluable information concerning the coagulation and adhesion phenomena of colloidal materials.

ACKNOWLEDGMENTS

REFERENCES

1. J. C. Giddings, Science, **260**, 1456 (1993).

2. K.D .Caldwell, Anal. Chem., **60**, 959A (1988).

3. A. Koliadima, E. Dalas, G. Karaiskakis, J. High Resol. Chromatogr., **13**, 338 (1990).

4. J. J.Kirkland, W. W. Yan, W. A. Doerner, J. W. Grand, Anal. Chem., **52**, 1944 (1980).

5. J. C. Giddings, F. J. F. Yang, M. N. Myers, Anal. Chem., **46**, 1917 (1974).

6. J. C. Giddings, K. D. Caldwell, "Field-Flow Fractionation," in **Physical Methods of Chemistry**, B. W. Rossiter, J. F. Hamilton, eds., John Wiley & Sons, New York, 1989, Vol. 3B, Chap. 8, p. 867.

7. M. Martin, P. S. Williams, "Theoretical Basis of Field-Flow Fractionation," in **Theoretical Advancement in Chromatography and Related Separation Techniques**, F. Dondi, G. Guiochon, eds., NATO ASI series C: Mathematical and Physical Science, Kluwer, Dordrecht, 1992, Vol. 383, p. 513.

8. D. Melucci, G. Gianni, G. Torsi, A. Zattoni, P. Reschiglian, J. Liq. Chromatogr. & Rel. Technol., **20**, 2615 (1997)

9. E. Urbankova, J. Chmelik, J. Liq. Chromatogr. & Rel. Technol., **20**, 2637 (1997).

10. G. Karaiskakis, A. Koliadima, Chromatographia, **28**, 31 (1989).

11. A. Koliadima, G. Karaiskakis, J. Chromatogr., **517**, 345 (1990).

12. E. Ruckenstein, A. Marmur, W. N. Gill, J. Colloid Interface Sci., **61**, 183 (1977).

13. R. Hogg, T. W. Healy, D. W. Fuersteuan, Trans. Faraday Soc., **62**, 1638 (1966).

14. P. C. Hiemenz, **Principles of Colloid and Surface Chemistry**, Marcel Dekker Inc., New York, 1977, p. 457.

15. A. Athanasopoulou, G. Karaiskakis, Chromatographia, **40**, 734 (1995).

16. A. Koliadima, G. Karaiskakis, Chromatographia, **39**, 74 (1994).

17. J. C. Giddings, G. Karaiskakis, K. D. Caldwell, M. N. Myers, J. Colloid Inter-face Sci., **92**, 66 (1983).

18. A. Koliadima, G. Karaiskakis, J. Liq. Chromatogr., **11**, 2863 (1988).

19. G. Karaiskakis, M. N. Myers, K. D. Caldwell, J. C. Giddings, Anal. Chem., **53**, 1314 (1981).

20. F-S. Yang, K. D. Caldwell, J. C. Giddings, J. Colloid Interface Sci., **92**, 81 (1983).

Request Permission or Order Reprints Instantly!

Interested in copying and sharing this article? In most cases, U.S. Copyright Law requires that you get permission from the article's rightsholder before using copyrighted content.

All information and materials found in this article, including but not limited to text, trademarks, patents, logos, graphics and images (the "Materials"), are the copyrighted works and other forms of intellectual property of Marcel Dekker, Inc., or its licensors. All rights not expressly granted are reserved.

Get permission to lawfully reproduce and distribute the Materials or order reprints quickly and painlessly. Simply click on the "Request Permission/Reprints Here" link below and follow the instructions. Visit the U.S. Copyright Office for information on Fair Use limitations of U.S. copyright law. Please refer to The Association of American Publishers' (AAP) website for guidelines on Fair Use in the Classroom.

The Materials are for your personal use only and cannot be reformatted, reposted, resold or distributed by electronic means or otherwise without permission from Marcel Dekker, Inc. Marcel Dekker, Inc. grants you the limited right to display the Materials only on your personal computer or personal wireless device, and to copy and download single copies of such Materials provided that any copyright, trademark or other notice appearing on such Materials is also retained by, displayed, copied or downloaded as part of the Materials and is not removed or obscured, and provided you do not edit, modify, alter or enhance the Materials. Please refer to our Website User Agreement for more details.

Order now!

Reprints of this article can also be ordered at
http://www.dekker.com/servlet/product/DOI/101081JLC100102058